

**THE CHANGES IN GROWTH AND COMPOSITION OF MARINE  
MICROALGAE IN RESPONSE TO SODIUM BICARBONATE AND  
NITROGEN**

An Undergraduate Research Scholar Thesis

by

MARCELLA M. NUNEZ

Submitted to Honors and Undergraduate Research  
Texas A&M University  
in partial fulfillment of the requirements for the designation as

UNDERGRADUATE RESEARCH SCHOLAR

Approved by  
Research Advisor:

Dr. Antonietta Quigg

May 2013

Major: Marine Science  
Minor: Chemistry

# TABLE OF CONTENTS

	Page
TABLE OF CONTENTS.....	1
ABSTRACT.....	3
DEDICATION.....	5
ACKNOWLEDGEMENTS.....	6
CHAPTER	
I INTRODUCTION.....	7
II MATERIALS AND METHODS.....	10
Cultivation of microalgae .....	10
Determination of Growth Rate.....	11
Photosynthetic performance of microalgae (FIRE) .....	11
Nile Red (NR) Fluorescence of microalgae .....	12
Biomass composition.....	13
Dry weight, ash content and ash free dry weight.....	13
Soluble protein content.....	13
CHN and crude protein content.....	14
FAME fatty acid determination.....	14
Sample preparation.....	14
Fatty Acid methyl Ester (FAME ) derivative preparation.....	15
GC/MS/FID.....	15
Epi-fluorescence Microscopy.....	16
Statistical Methods.....	16
III RESULTS.....	17
Growth rates under different concentrations of NaHCO <sub>3</sub> .....	17
Photosynthetic performance.....	19
Lipid changes (Oil indexes) in <i>N.salina</i> and <i>P. tricornutum</i> based on Nile Red 21	

AFDW, DW, ash content, crude protein, and soluble protein.....	22
Carbon (C %), Nitrogen (N %), and Carbon-Nitrogen Ratio (C: N).....	23
Epi-fluorescence Microscope.....	25
Lipid and Fatty Acid Composition.....	26
IV DISCUSSION.....	28
REFERENCES.....	34

## ABSTRACT

The changes in growth and composition of marine microalgae in response to sodium bicarbonate and nitrogen. (May 2013)

Marcella M. Nunez  
Department of Marine Science  
Texas A&M University

Research Advisor: Dr. Antonietta Quigg  
Department of Marine Biology

Currently biofuel is produced from plants as well as microbes. The oils, carbohydrates or fats generated by these organisms are refined to produce biofuel. Algae (phytoplankton) can be converted directly into energy and therefore can be a source of renewable energy. In this biofuels research, two marine phytoplankton (*Phaeodactylum tricornutum* and *Nannochloropsis salina*) were grown in f/2 medium with various sodium bicarbonate ( $\text{NaHCO}_3$ ) concentrations (0, 0.5, 1.0, 2.0, 5.0  $\text{g L}^{-1}$ ) during the growth phase (GP) and lipid phase (LP). In order to increase the amount of oil produced, the phytoplankton were nitrogen (N) limited during the LP. Effects of  $\text{NaHCO}_3$  concentrations and N-limitation on growth and biochemical composition of the diatom *P. tricornutum* and the green alga *N. salina* were investigated. The average growth rate in *P. tricornutum* is  $0.102 \pm 0.006 \text{ d}^{-1}$  for concentrations of 0.0 to 2.0  $\text{g L}^{-1} \text{NaHCO}_3$  except for 5.0  $\text{g L}^{-1}$  which was  $0.223 \pm 0.013 \text{ d}^{-1}$ . For *N. salina*, growth rates were generally  $0.20 \pm 0.006 \text{ d}^{-1}$  for concentrations of 0.0 to 2.0  $\text{g L}^{-1} \text{NaHCO}_3$  except for 5.0  $\text{g L}^{-1}$  which was higher,  $0.256 \pm 0.019 \text{ d}^{-1}$ . The relative lipid content, exhibited as the highest oil index value, was in 5.0  $\text{g L}^{-1} \text{NaHCO}_3$  for both species in LP. The variations at lower concentrations indicate species-specific responses

to changing  $\text{NaHCO}_3$  conditions. The preliminary findings reveal the importance of considering  $\text{NaHCO}_3$  as a supplemental C source in the culturing marine phytoplankton in large scale production of biofuels.

## **DEDICATION**

This work is dedicated to my family and my husband for their support.

## **ACKNOWLEDGEMENTS**

This work is the result of research funded by Undergraduate Research Scholar Program, Welch Foundation, Texas Institute of Oceanography, and the Texas Sea Grant. Texas Agrilife Research Center in Pecos, TX (Lou and Jola Brown) is thanked for their support in performing the lipid analysis. I would like to thank the support the members of the Phytoplankton Dynamics Laboratory, especially Matthew Gore and Yuelu Jiang. The following undergraduate students assisted in various aspects of the study: Salem Harry, Hanna Preschel, Lauren Cucci and Jocelyn Bosquez. I especially would like to thank the support and guidance of my research advisor Dr. Antonietta Quigg.

# CHAPTER I

## INTRODUCTION

Microalgae are a diverse group of prokaryotic and eukaryotic photosynthetic microorganisms that can grow rapidly due to their simple cellular structure. More importantly, algae can be converted into several different types of renewable biofuels, including green diesel, jet fuel, methane (biogas), ethanol, butanol, as well as a variety of co products (Singh *et al.*, 2010). The idea of using microalgae as a source of fuel is not new but it is now being taken seriously because of the escalating price of petroleum and concerns about climate change associated with burning fossil fuels (Chisti 2007). Our reliance on fossil fuels has caused CO<sub>2</sub> enrichment into the atmosphere which contributes not only to global warming but also to other impacts on the environment and human life. One of the main purposes of replacing oil-derived fuels and products with bio-based fuels and chemicals is to reduce the net carbon emissions.

One of the key reasons why these single celled photosynthetic organisms, the microalgae, are considered as feedstock for oil is their rapid growth rate, high energy content and hence high oil yield. Some algal strains are capable of doubling their mass several times per day. In some cases, more than half of that mass consists of lipids or triacylglycerides (Achara, 2012). The per unit area yield of oil from algae is estimated to be from 20,000 to 80,000 L per acre, per year; this is 7–31 times greater than the next best crop, palm oil (Demirbas *et al.*, 2011). Biodiesel from algae seems to be the only renewable biofuel that has the potential to completely displace petroleum-derived transport fuels without adversely affecting supply of food and other crop products



(Christi *et al.*, 2008). Current studies suggest that average biodiesel production yield from microalgae is 10-20 times higher than the yield obtained from various crop plants (Chisti 2007).

Since microalgae are so diverse and vary from species to species on the types of lipids and complex oils produced it hard to determine which species is the best. Over the decades there has been a vast amount of research done on numerous phytoplankton species to determine which one would produce the largest biomass for cultivation. In research there are various ways to alter the parameters in the search for optimal production needs. For instance,  $\text{NaHCO}_3$  is a good source of inorganic carbon and can be used in the photosynthetic production in algae. In the field of biofuels and algal research, it is an alternative inorganic carbon source which is used in culture medium. In the laboratory, as well as large scale cultivation,  $\text{NaHCO}_3$  comes as a cheaper solution than  $\text{CO}_2$  (gas source). The role of  $\text{NaHCO}_3$  in algal cultivation has long been a subject of intensive experimental work, but there has been no general agreement on the mechanisms by which  $\text{NaHCO}_3$  contributes to overall cultivation of microalgae and how it might affect the key parameters, such as algal growth, biomass productivity and lipid production. Nutrients are another important factor and for the biofuels industry in the production of biomass. Nutrient availability is of considerable importance to the growth and primary production of microalgae.

Typical nutrient limitation in nature includes the supply of nitrogen, phosphate, and/or silicate (diatoms) (Berges *et al.*, 1998, Geider *et al.*, 1996). Nitrogen, unlike phosphorous, is not limited in supply but is often a limiting macronutrient when it comes to plant and algae growth. Algae require nitrogen to be fixed into ammonia, nitrates and similar molecules, in order to be used as a nutrient source (Hannon, 2010). Phytoplankton cells undergoing nutrient limitation change their

cellular composition; N limitation can lead to a decrease in protein content and a relative increase in carbohydrate and/or lipid storage (Giordano *et al.*, 2001, Dean *et al.*, 2010). N limitation can also result in a decrease in growth rate and photosynthetic efficiency (Parkhill *et al.*, 2001). The biochemical changes measured in microalgae reflect their mechanisms for coping with the changes of physiological parameters and are known to be species-specific (Jiang *et al.*, 2012).

The two marine microalgae, *Phaeodactylum tricornutum* (diatom) and *Nannochloropsis salina* (green algae) will be used to examine the role of sodium bicarbonate ( $\text{NaHCO}_3$ ) at 0, 0.5, 1.0, 2.0, and 5.0  $\text{gL}^{-1}$  in f/2 medium during the growth phase (GP) and lipid phase (LP). The research will examine how  $\text{NaHCO}_3$  can influence the growth rate and biochemical composition of the marine microalgae in both the GP and LP. In our preliminary findings, we found that the marine algae treated with the higher levels of  $\text{NaHCO}_3$  will produce higher biomass and cellular lipid production due to the increased available amount of carbon for photosynthesis and growth. It furthermore indicates species-specific responses to changing  $\text{NaHCO}_3$  conditions on growth and oil production in a complex manner. This study will build on findings from previous works by investigating the effects of different levels of  $\text{NaHCO}_3$  in microalgae cultures for biofuel production.

## CHAPTER II

### MATERIALS AND METHODS

#### **Cultivation of the microalgae**

*Phaeodactylum tricornutum* (UTEX 646) and *Nannochloropsis salina* (CCMP 1776) were grown in f/2 medium (Guillard and Ryther, 1962; Guillard, 1975) with natural seawater acquired from the Gulf of Mexico (off the coast of Texas) and filtered through 0.45  $\mu\text{m}$  membrane to remove particulates before starting experiments. Media was sterilized in one of two ways: (i) by autoclaving (121°C, 40 min) or (ii) by double filtration. For the latter, media were filtered through a Millipore disposable groundwater 0.45 $\mu\text{m}$  pore size filter into an acid washed carboy, and then into an autoclaved sterilized carboy. Once sterilized, the media was allowed to acclimate to the experimental temperatures before use. The two species were grown in triplicate 500 mL polycarbonate bottles at  $19 \pm 1^\circ\text{C}$  under a 12 h:12 h light:dark cycle. The light intensity ranged between 130 and 150  $\mu\text{mol photons m}^{-2} \text{ s}^{-1}$ . (Li-Cor, Nebraska, USA; LI-1888 integrating quantum radiometer photometer). The cultures were inoculated from semi-continuous batch cultures which were growing in exponential phase prior to the experiment in order to assess the possibility of a larger scale replicate experiment. The two algae cultures were shaken gently three times a day to ensure continuous mixing and keep the algae in suspension, In all cases, algae were acclimated to the treatment conditions (temperatures, light:dark cycle and medium) for ~3 generations before starting experiments.

In the experiment, analytical grade  $\text{NaHCO}_3$  was used (Sigma-Aldrich, USA), a solution stock 50g  $\text{L}^{-1}$  of  $\text{NaHCO}_3$  was prepared using sterilized natural seawater, and then double filtered

through a 0.45 $\mu\text{m}$  pore size filter using a sterilized interchangeable filtering capsule. Final concentrations of  $\text{NaHCO}_3$  were added to the media as 0, 0.5, 1.0, 2.0, 5.0  $\text{gL}^{-1}$  in triplicates in the acclimation and both experimental phases (GP and LP). After cultures reached stationary phase, cultivation was continued into lipid formation phase, that is, half of the culture was replaced with fresh media lacking N but with the same  $\text{NaHCO}_3$  concentrations as growth experiment to induce lipid formation. Cultures were monitored as during the growth phase.

### **Determination of Growth Rates**

Experiments were conducted in semi-continuous batch mode. Algal growth was monitored by daily changes in  $\text{OD}_{750}$  with a spectrophotometer (UV-2501PC UV-VIS, Shimadzu). Fresh media was used as blank measurements. The relative growth rate was calculated from  $\text{OD}_{750}$  measurements:  $\mu = 1/T (\ln N_{t+1} - \ln N_t) \text{ days}^{-1}$ , where  $N_t$  is the  $\text{OD}_{750}$  reading at time point t,  $N_{t+1}$  is the  $\text{OD}_{750}$  reading at time point t+1, and T (days) is the interval between observations. On day 0, each culture was inoculated at a cell density equivalent to an optical density at 750 nm ( $\text{OD}_{750}$ ) between 0.3 and 0.5. Thereafter,  $\text{OD}_{750}$  was measured once a day. After the exponential growth phase, half of the volume was harvested and replaced with fresh media lacking N. This process was repeated only once during the transition to the lipid phase. Growth rates from the last growth cycle were used for final statistical analyses.

### **Photosynthetic performance of microalgae (FIRE)**

After measuring  $\text{OD}_{750}$ , samples were then measured using a Fluorescence Induction and Relaxation (FIRE) (Satlantic Instruments S/N 2) system. All measurements were performed using a gain of 400 to 2400 and 30 acquisitions. We used only information collected from the single

turnover (ST) component of the transient (Revellame *et al.*, 2010), specifically; the minimal and maximal fluorescence yields ( $F_{O(ST)}$  and  $F_{M(ST)}$  respectively) were obtained on dark acclimated (min. 30 min) samples. Variable fluorescence (FV) was calculated as the difference between these parameters [ $F_{M(ST)}$  and  $F_{O(ST)}$ ]. The efficiency of photosystem II (PSII) defined as the maximum change in the quantum yield of photochemistry was calculated as  $F_V/F_{M(ST)} = [F_{M(ST)} - F_{O(ST)}]/F_{M(ST)}$ . Ratio below 0.40 is considered unhealthy while a ratio of 0.65 is considered healthy. Fresh medium was used to correct for interference from background fluorescence. The blank usually contributed <10% of the signal. The functional absorption cross section for PSII ( $\sigma_{PSII}$ ;  $\text{\AA}^2 \text{ quanta}^{-1}$ ), the minimum turnover time of electron transfer between reaction centers ( $\tau_{Qa}$ ;  $\mu\text{sec}$ ) and the connectivity factor ( $p$ ; unitless) were derived using the systems software.

### **Nile Red (NR) Fluorescence of microalgae**

The changes of intracellular neutral lipid during the lipid formation experiment were followed by changes in fluorescence intensity of NR stained cultures as described previously (Cooksey *et al.*, 1987, Elsey *et al.*, 2007) with modifications described in Jiang *et al.* Cells were stained with  $250 \mu\text{gml}^{-1}$  NR (final concentration,  $0.75 \mu\text{gml}^{-1}$ ) (9-diethylamino-5H-benzophenoxazine-5-one) solution in acetone and measured by spectrofluorophotometer (RF-5301, Shimadzu) using a 490 nm excitation and 500-750 nm emission wavelengths. The relative fluorescence intensity of NR was obtained after subtraction of the self-fluorescence of NR. The relative NR fluorescence intensity is then normalized for cell density using OD750 nm as lipid index (Eq. 1)

$$\text{Lipid index} = \frac{\text{Total area calculated under 580 nm peak}}{\text{Absorbance measured at OD750 nm}} \quad (\text{Eq. 1})$$

## **Biomass Composition**

### **Dry weight, ash content and ash free dry weight**

Ash free dry weight (AFDW) and dry weight (DW) were used to measure the algal biomass. AFDW is an indicator of the organic carbon content in the sample. Algal cultures were filtered onto precombusted (500 °C, 4hours) glass-fiber filters (Whatman GF/F, 47mm, nominal pore size 0.7 µm) and rinsed with a solution of 0.34 N NaCl in 0.1 N HCl to remove the bicarbonate, followed by a rinse with 0.435M ammonium formate to remove the NaCl (Britton *et al.*,1987; Zhu *et al.*,1997). Samples were dried at 103-105 °C for 2 hours. They were then stored in desiccators containing valid desiccant to ensure they remained dry and were weighed with a microbalance (XS105, Mettler Toledo). The microbalance was situated in an air-conditioned room to ensure that samples would not hydrate due to variable humidity. Aluminum dishes containing silica gel were placed inside the microbalance to ensure any moisture present would not cause hydration of the sample, and weighed again. After dry weights were measured, the samples were ashed at 500 °C for 4h. Ash weight were measured the same as mentioned above. AFDW was calculated by subtracting the ash weight from the total DW. Ash content was expressed as the percentage of ash weight in the total DW.

### **Soluble protein content**

For analysis of soluble protein content, algal cultures were collected (2mL) and stored in the -20°C freezer till analysis. SDS (final concentration 0.5%) was added at room temperature and the sample was thoroughly vortexed and sonicated in an ice bath for 15 min. After centrifugation (4,000g, 15 min), the soluble protein in the supernatant was measured by using the Pierce BCA or micro BCA protein assay kit (#23225 and 23227).

### **CHN and crude protein content**

Samples (20 mL) were collected using an acid washed syringe (polyethylene barrels and polypropylene plungers) and filtered onto precombusted 25 mm Whatman GF/F membranes (500<sup>0</sup>C, 4hr). For CHN, algal cultures were collected and stored in the -20<sup>0</sup>C freezer till analysis. The filtered algal samples were analyzed with a CHN analyzer (PerkinElmer 2400 CHNS/O Analyzer). The combustion temperature was set at 925<sup>0</sup>C and the reduction tube was set at 640<sup>0</sup>C. The analyzer was conditioned before sample analysis by running successive blank and external standard samples until the carbon (C), hydrogen (H), and nitrogen (N) outputs stabilized. Acetanilide was used as external standard. Crude protein was estimated by multiplying the N content, which was normalized to AFDW, by 6.25 (Heydeman, 1973).

### **FAME fatty acid determination**

#### **Sample preparation**

Algal culture for fatty acid analysis was filtered onto precombusted 47mm Whatman GF/F membranes (500<sup>0</sup>C, 4hr). The sides of the filter funnels were washed any residual algae with DI water. Filters were stored in the -20<sup>0</sup>C freezer until analysis. The fatty acid profile of the oil sample was determined by converting the fatty acids in the oil to fatty acid methyl esters (FAMES).

#### **FAMES derivative preparation**

Fatty acid methyl esters (FAMES) were prepared by a modified acid transesterification as described by (Christie, 2003, Dahmer *et al.*,2007, O'Fallon *et al.*,1989).Briefly, the GF/F filters

with algal cells were incubated with the transesterification reagents (recorded volume of standard C15), 6 ml of 4% (v/v) H<sub>2</sub>SO<sub>4</sub> in methanol for 1 hour at 103°C with continuous mixing for producing FAMES (Revellame *et al.*, 2010). The solution was allowed to cool to room temperature, vortex for 1 minute and then the FAMES were extracted with 7 ml of water: hexane (4:3) (Gunawan *et al.*, 2011). Vigorous mixing was done again by vortex for 1 minute and the samples were transferred in to small vials for extraction by centrifuged at 3500 rpm for 30 min for phase separation. After separation recorded measurements of the hexane phase (approx. 0.5 μL) was collected and the addition of C13/C19 FAME (approx. 0.05 μL) was added to small vials for GC-MS analysis.

#### **Gas Chromatography-Mass Spectrometry- Flame Ionization Detector (GC-MS/FID)**

The FAME composition was determined using an Agilent 7890A gas chromatography (GC) , 5975B mass spectrometer (MS) (Agilent, Palo Alto, CA) with automatic injector (Agilent 7683B automatic liquid sampler), and a Dean splitter to utilize both flame ionization detector (FID) and mass spectrometric detector (MSD) detectors on one column. The GC-MS was equipped with a DB-WAX capillary column (length: 30m; ID: 0.25 mm). The column was held at 150 °C for 1 min, ramped 160 °C at 10 °C/min, then to 210 °C at 15 °C/min, finally to 250°C at 20 °C/min. The total run time for the analysis method was 21.3 min. The injector was kept as 220°C with an injection volume of 1 μL under split mode (50:1). The FID temperature was set at 300°C. The transfer line between GC and MS was kept at 280 °C. Helium (>99%, CAS 110-54-3) was used as the carrier gas with a flow rate of 1.3 mL/min. The quantities of individual FAMES were identified and estimated from the retention time and peak areas on the chromatogram using authentic standards (Nu-Chek-Prep reference standard mix, GLC-68A).



Efficiency of the fatty acid methylation step of algae samples was using pentadecanoic acid (C15:0; Fluka, 1382992) as the internal standard (Glaser et al., 2010; Peydecastaing et al., 2009; Lepage et al., 1988). The results are reported as %lipid of lipid after normalization to AFDW.

### **Epifluorescence Microscopy**

*P. tricornutum* and *N. salina* were viewed under epifluorescence microscope (Zeiss, Model), excitation: 488 nm; emission: 500 –570 nm at both 0.0 and 5.0g L<sup>-1</sup>NaHCO<sub>3</sub> after Nile Red staining in order to differentiate the effects of increasing concentrations at 1000x magnification.

### **Statistical Methods**

Each experiment was performed in triplicate. Data represent means ± standard deviations (SD).

## CHAPTER III

### RESULTS

#### Growth rates under different concentrations of NaHCO<sub>3</sub>

The growth rates followed by changes in optical density at 750nm (OD<sub>750</sub>; relative units) of *P. tricornutum* and *N. salina* were recorded into exponential phase of GP and LP (~ 10-12 days, respectively; Figure 1A, 1C). For both species in GP, there was a lag phase of (2-3 days) in all concentrations of bicarbonate. *P. tricornutum* had growth rates of  $0.338 \pm 0.02$  for concentrations of 0.5, 1.0 and 2.0 g L<sup>-1</sup> NaHCO<sub>3</sub> except for 0.0 g L<sup>-1</sup> which was much lower,  $0.195 \pm 0.02$  (Figure 1A). In all concentrations of NaHCO<sub>3</sub>, except 0.0 g L<sup>-1</sup> which slowed in biomass, OD<sub>750</sub> biomass significantly increased overall for *P. tricornutum*. For *N. salina*, growth increase exponentially throughout the exponential phase from 0.0 to 5 g L<sup>-1</sup> (Figure 1C) with growth rates from  $0.192 \pm 0.015$  to  $0.659 \pm 0.018$ . The final GP OD<sub>750</sub> readings were significantly higher in *N. salina* in 5 g L<sup>-1</sup> at  $0.659 \pm 0.018$ , and decreased in order of NaHCO<sub>3</sub> concentration in the culture.

After reaching the stationary phase both species were transferred into N-free media. Growth rates slowed overall but still increased in density throughout the LP (~10-12days; Figure 1B, 1D). *P. tricornutum* had the highest OD<sub>750</sub> of  $0.649 \pm 0.018$  for concentrations of 0.5 g L<sup>-1</sup> NaHCO<sub>3</sub> except for 0.0 g L<sup>-1</sup> which was lower from  $0.323 \pm 0.014$ . For concentrations 2.0 and 5.0 g L<sup>-1</sup>, biomass increased; however, for concentrations 1.0 g L<sup>-1</sup>, biomass dropped below the control (0.0 g L<sup>-1</sup> NaHCO<sub>3</sub>; Figure 1B). It is not clear why this one treatment behaved differently to all other treatments. *N. salina* highest growth remained 5.0g L<sup>-1</sup> at  $0.937 \pm 0.01$ , while  $0.838 \pm 0.02$

for concentrations of 0.5 and 2.0 g L<sup>-1</sup> NaHCO<sub>3</sub> except for the control, 0.0 g L<sup>-1</sup> which was significantly lower from 0.372±0.03 (Figure 1D).

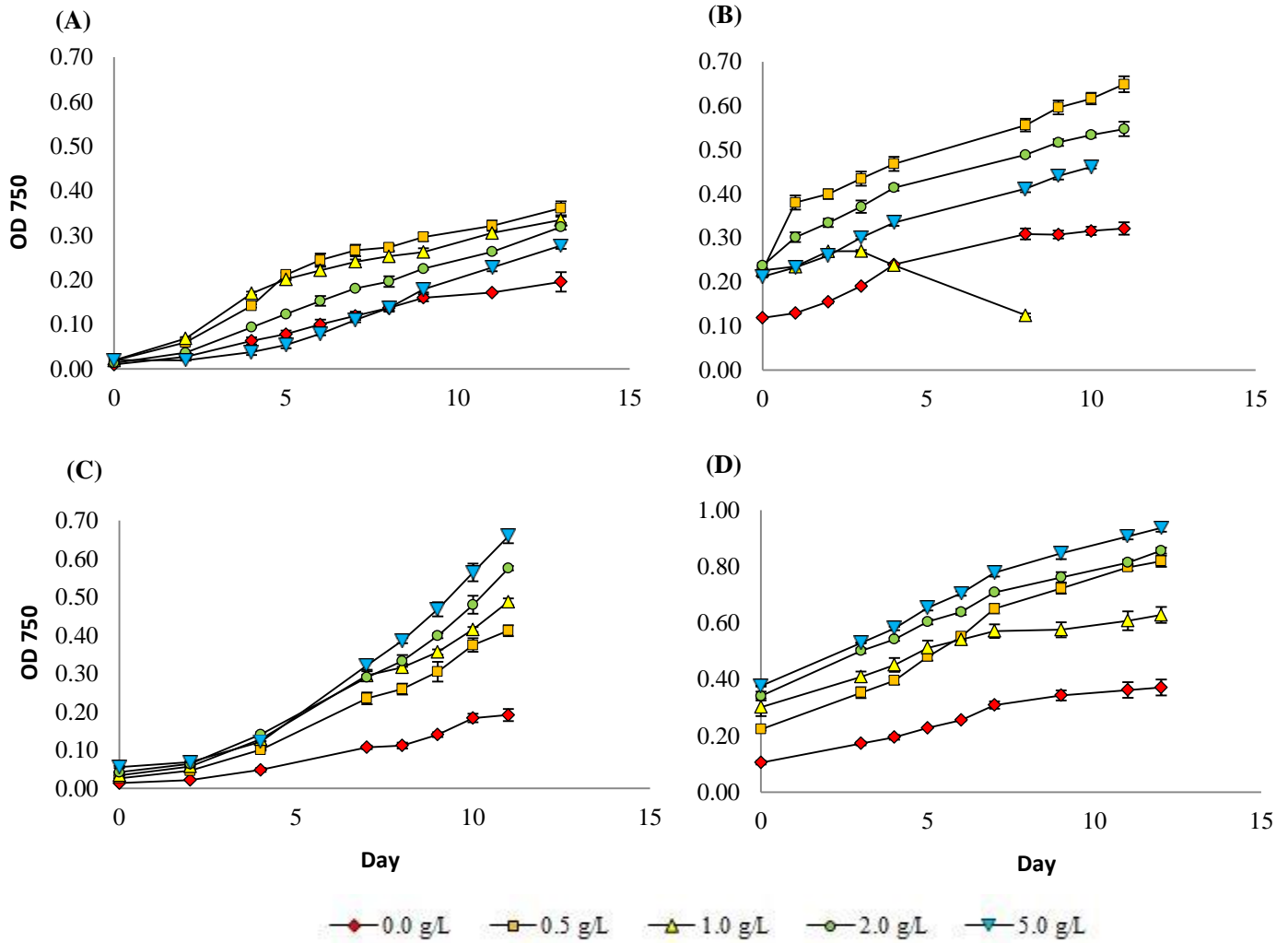


Figure 1: OD<sub>750</sub> Growth rates during the GP, growth phase, and LP, lipid formation phase. (A) *P. tricornutum*- GP, (B) *P. tricornutum* - LP, (C) *N. salina* - GP, and (D) *N. salina* - LP. Errors bars represent standard deviation (n=3). If the error bars are not visible, they are smaller than the symbol.

## Photosynthetic performance

The photosynthetic activity ( $F_v/F_m$ ) of algal cells grown under N-replete (GP) and N-free (LP) media showed *P. tricornutum* and *N. salina* behaved differently (Figure 2). During both phases  $F_v/F_m$  values were on average  $0.622 \pm 0.004$  (GP) and  $0.539 \pm 0.006$  (LP) during exponential phase for *N. salina* respectively (Figure 2C, 2D). While during the GP, the  $F_v/F_m$  for *P. tricornutum* peaked at day 2 in all concentrations of  $\text{NaHCO}_3$ ,  $0.578 \pm 0.005$  (Figure 2A). Then  $F_v/F_m$  gradually decreased at different rates per concentration during the exponential phase to values of  $0.289-0.482 \pm 0.004$ . Under N-free,  $F_v/F_m$  values for *P. tricornutum* increased in all concentration of  $\text{NaHCO}_3$  to a normal ratio of  $0.492 \pm 0.01$  (Figure 2B).

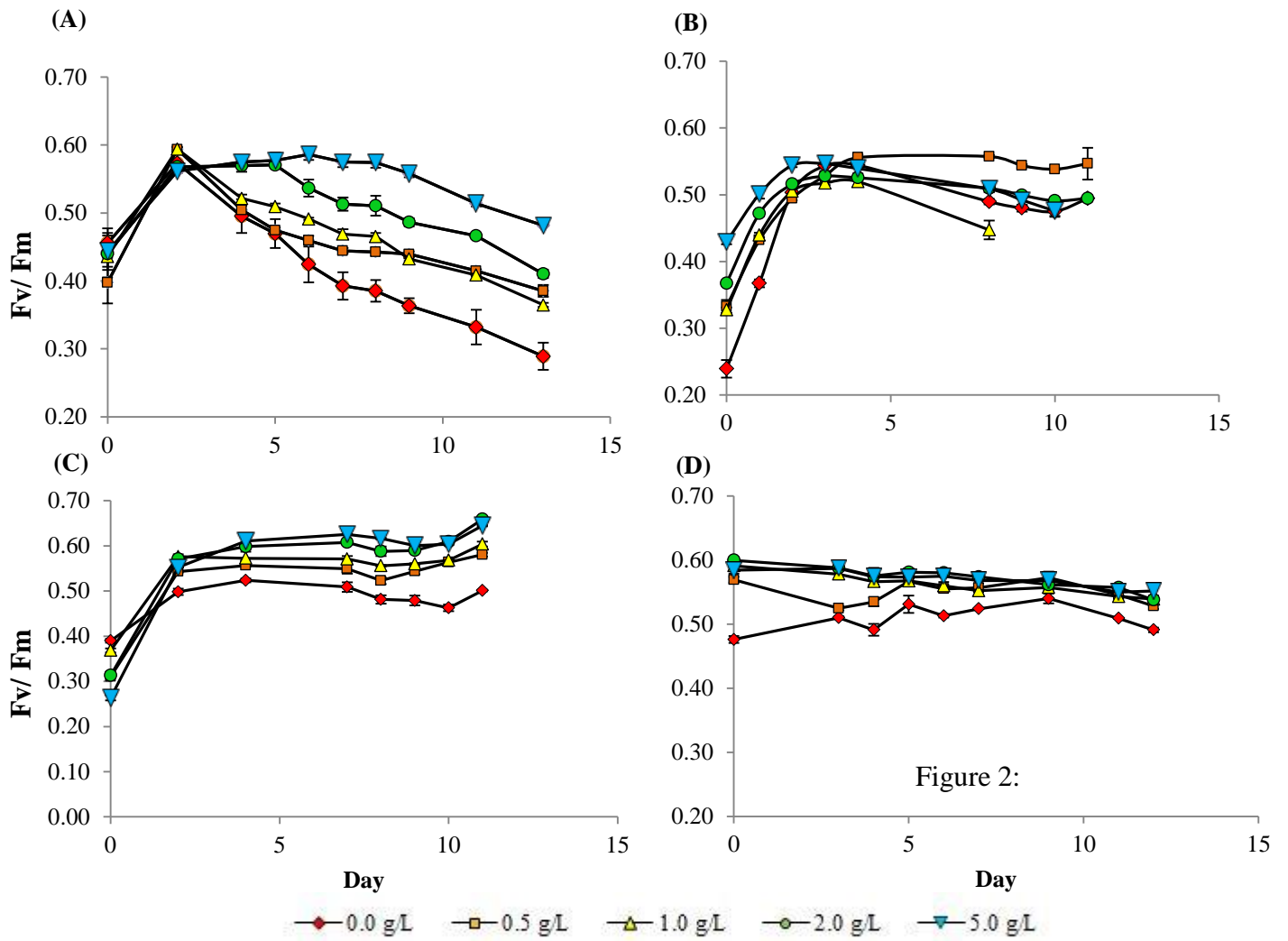


Figure 2: Photosynthetic activity of (A) *P. tricornutum* - GP, (B) *P. tricornutum* - LP, (C) *N. salina*-GP, and (D) *N. salina* - LP. Errors bars represent standard deviation (n=3). If the error bars are not visible, they are smaller than the symbol.

### Lipid changes (Oil indexes) in *N. salina* and *P. tricornutum* based on Nile Red (NR)

Both species in N-replete media (GP) showed no variation in lipid production during the exponential phase (Figure 3A, 3C). For *P. tricornutum*, lipid indices remained relatively close in 0.0, 0.5, 1.0, and 2.0 g L<sup>-1</sup> NaHCO<sub>3</sub> in the LP, except for 5.0 g L<sup>-1</sup> significantly higher (Figure 3B). Although lipid indices of *N. salina* in all concentrations of NaHCO<sub>3</sub> greatly exceeded the lipid production of the control treatment during the LP of *P. tricornutum* (Figure 3D). After 4 days incubation in the LP, supplement of 5.0 g L<sup>-1</sup> NaHCO<sub>3</sub> in *N. salina* produced the highest oil index in order of decreasing NaHCO<sub>3</sub> concentration (Figure 3D).

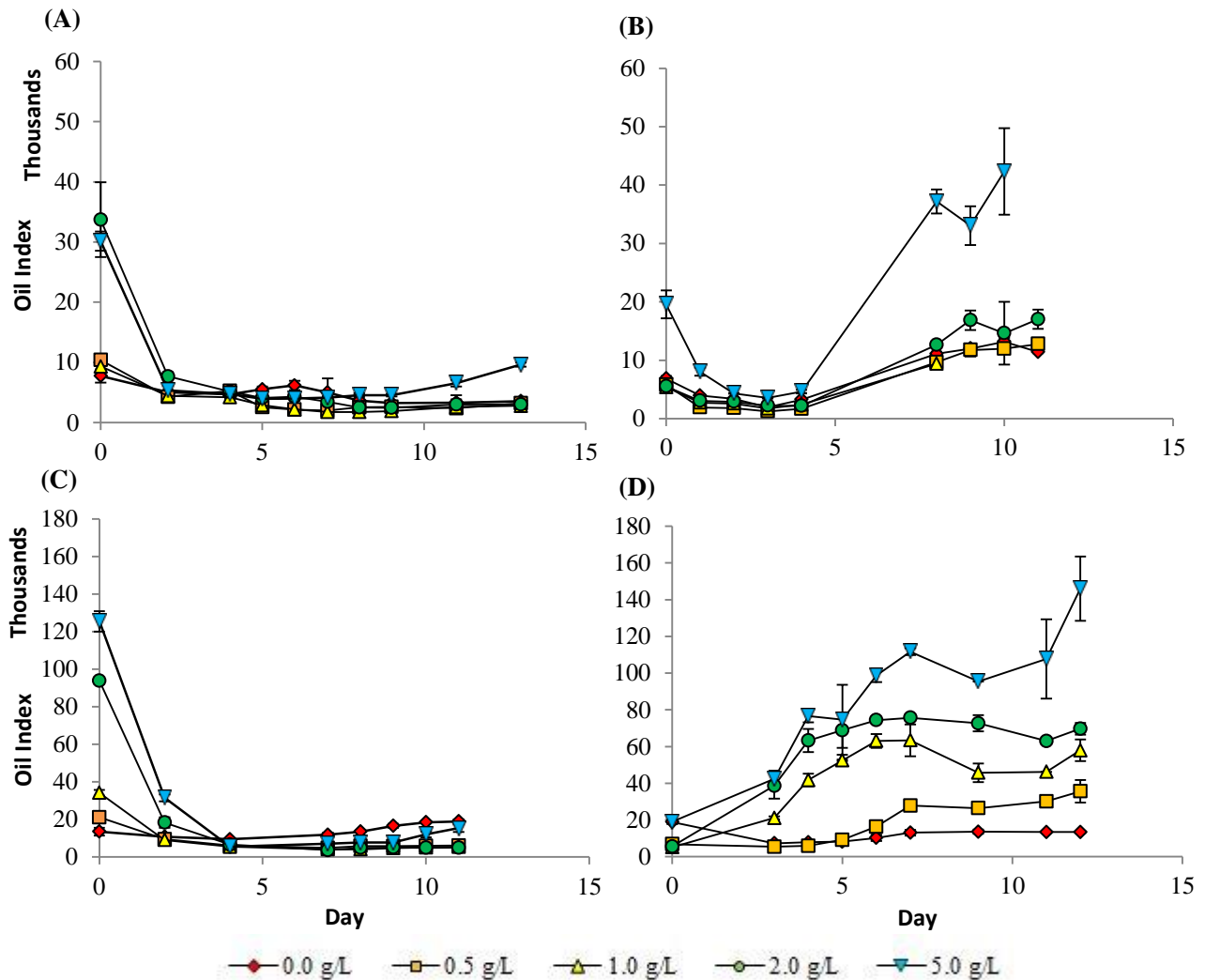


Figure 3: Lipid changes (Oil indexes) based on Nile Red (NR). (A) *P. tricornerutum* - GP, (B) *P. tricornerutum* - LP, (C) *N. salina* - GP, and (D) *N. salina* - LP. Errors bars represent standard deviation (n=3). If the error bars are not visible, they are smaller than the symbol.

### **AFDW, DW, ash content, crude protein, and soluble protein**

AFDW ( $\text{g L}^{-1}$ ), Dry weights (DW), ash content ( $\%$ ,  $\text{g g}^{-1}$  DW), crude protein ( $\%$ ,  $\text{g g}^{-1}$  AFDW), and soluble protein ( $\text{mg/g}$  AFDW) of *N. salina* and *P. tricornerutum* in the five concentrations of  $\text{NaHCO}_3$  media are shown in Table 1. During the growth phase the maximum biomass (DW) achieved for *N. salina*,  $0.308 \pm 0.04 \text{ g L}^{-1}$  in  $0.5 \text{ NaHCO}_3 \text{ g L}^{-1}$ . For *P. tricornerutum*,  $0.404 \pm 0.037 \text{ g L}^{-1}$  was measured in  $0.0 \text{ g L}^{-1} \text{ NaHCO}_3$ , the highest DW (Table 1). An alternative indicator for biomass production, AFDW, demonstrated in the GP, the highest overall ash contents were in for both species were in the  $0.0 \text{ g L}^{-1} \text{ NaHCO}_3$ : *N. Salina*  $58 \pm 2.5\%$  and *P. tricornerutum*  $38 \pm 16\%$ . The highest crude protein content ( $\%$ ,  $\text{g g}^{-1}$  AFDW) measured: *N. salina* was  $78 \pm 2.9\%$  in  $2.0 \text{ g L}^{-1} \text{ NaHCO}_3$ . While for *P. tricornerutum* highest crude protein measurements were in  $1.0 \text{ g L}^{-1}$  and  $2.0 \text{ g L}^{-1} \text{ NaHCO}_3$  at  $81 \pm 4.9\%$  and  $81 \pm 4.1 \%$  respectively. In addition, soluble protein content for *N. salina*,  $24.16 \pm 3.3 \text{ mg/g}$  AFDW in  $5.0 \text{ g L}^{-1} \text{ NaHCO}_3$  medium, but higher for *P. tricornerutum*,  $33.6 \pm 6.9 \text{ mg/g}$  AFDW in  $5.0 \text{ g L}^{-1}$ .

For *N. salina*, the highest DW was  $0.706 \pm 0.01 \text{ g L}^{-1}$  measured at the end of lipid formation phase was observed in the treatment with  $0.5 \text{ g L}^{-1} \text{ NaHCO}_3$ . For *P. tricornerutum* the highest AFDW,  $0.338 \pm 0.012 \text{ g L}^{-1}$  was in the treatment with  $0.5 \text{ g L}^{-1} \text{ NaHCO}_3$  and the highest DW of  $0.575 \pm 0.04 \text{ g L}^{-1}$  in the same  $\text{NaHCO}_3$  concentration during the lipid formation phase (Table 1).

The highest crude protein content (% , g g<sup>-1</sup>AFDW) measured: *N. salina* 80 ± 3.2% in 5.0 g L<sup>-1</sup> NaHCO<sub>3</sub>. While *P. tricornutum* highest crude protein measurements were in 2.0 g L<sup>-1</sup> and 5.0 g L<sup>-1</sup> NaHCO<sub>3</sub> at 98 ± 2.7% and 98 ± 2.7 %. In addition, soluble protein content for *N. salina*, decreased in lipid formation to 19.83 ± 2.98 mg/g AFDW in 2.0 g L<sup>-1</sup> NaHCO<sub>3</sub> medium, *P. tricornutum*, 15.24 ± 1.10 mg/g AFDW in 0.5 g L<sup>-1</sup> and 14.45 ± 0.77 mg/g AFDW in 0.5 g L<sup>-1</sup> NaHCO<sub>3</sub> (Table 1).

Species	Treatment									
	0 g L <sup>-1</sup> NaHCO <sub>3</sub>		0.5 g L <sup>-1</sup> NaHCO <sub>3</sub>		1 g L <sup>-1</sup> NaHCO <sub>3</sub>		2 g L <sup>-1</sup> NaHCO <sub>3</sub>		5 g L <sup>-1</sup> NaHCO <sub>3</sub>	
	GP	LP	GP	LP	GP	LP	GP	LP	GP	LP
<b>Dry weight (g L<sup>-1</sup>)</b>										
<i>N. salina</i>	0.277 ± 0.017	0.462 ± 0.053	0.308 ± 0.041	0.706 ± 0.005	0.220 ± 0.042	0.517 ± 0.110	0.198 ± 0.008	0.326 ± 0.024	0.233 ± 0.018	0.390 ± 0.022
<i>P. tricornutum</i>	0.404 ± 0.037	0.217 ± 0.005	0.184 ± 0.02	0.575 ± 0.04	0.331 ± 0.084	—	0.311 ± 0.08	0.464 ± 0.02	0.200 ± 0.03	0.355 ± 0.007
<b>Ash % DW (g g<sup>-1</sup>)</b>										
<i>N. salina</i>	58.18 ± 2.52	45.72 ± 0.912	53.35 ± 2.57	39.66 ± 0.74	36.36 ± 6.69	38.94 ± 7.06	25.93 ± 0.91	23.02 ± 1.55	29.88 ± 1.71	24.48 ± 3.676
<i>P. tricornutum</i>	38.50 ± 16.1	35.48 ± 1.53	21.61 ± 3.42	41.23 ± 2.31	34.28 ± 3.76	—	30.08 ± 8.12	52.89 ± 0.37	25.08 ± 4.87	39.48 ± 2.03
<b>soluble protein (mg g<sup>-1</sup>)</b>										
<i>N. salina</i>	4.92 ± 0.61	3.69 ± 0.54	6.63 ± 0.87	3.56 ± 0.24	18.26 ± 5.75	6.86 ± 2.64	20.94 ± 13.40	19.83 ± 2.98	24.16 ± 3.31	18.16 ± 3.35
<i>P. tricornutum</i>	3.87 ± 1.26	10.34 ± 1.05	31.93 ± 4.83	8.05 ± 1.55	15.24 ± 1.10	—	19.56 ± 4.18	8.35 ± 0.26	33.63 ± 6.97	14.45 ± 0.77
<b>Crude protein content % AFDW (g g<sup>-1</sup>)</b>										
<i>N. salina</i>	31.25 ± 1.37	30.41 ± 3.05	46.84 ± 0.66	42.56 ± 3.84	62.80 ± 1.24	57.82 ± 3.92	61.31 ± 9.0	68.02 ± 1.53	78.38 ± 2.97	80.19 ± 3.18
<i>P. tricornutum</i>	31.25 ± 5.14	31.63 ± 2.04	48.16 ± 5.55	90.15 ± 6.69	81.39 ± 4.99	—	81.58 ± 4.08	98.94 ± 2.68	77.07 ± 12.23	97.78 ± 2.69

Table 1: Changes in dry weight, ash% DW, soluble protein, and crude protein content of *N. salina* and *P. tricornutum* from growth to lipid formation media. Errors bars represent standard deviation (n=3).

### Carbon (C %), Nitrogen (N %), and Carbon-Nitrogen Ratio (C: N)

To further study the effect of NaHCO<sub>3</sub> concentrations, cellular carbon and nitrogen were measured and C: N ratios were compared (Table 2, Figure 4). The highest C% achieved in GP :



*N. salina*  $53.4 \pm 3.32$  in  $5.0 \text{ g L}^{-1}$   $\text{NaHCO}_3$  supplement and *P. tricornutum*  $83.4 \pm 3.0$  in  $1.0 \text{ g L}^{-1}$   $\text{NaHCO}_3$  supplement. In relation highest N % achieved in GP : *N. salina*  $8.31 \pm 0.49$  in  $5.0 \text{ g L}^{-1}$   $\text{NaHCO}_3$  supplement and *P. tricornutum*  $7.52 \pm 0.11$  in  $1 \text{ g L}^{-1}$   $\text{NaHCO}_3$  supplement. The highest C:N ratio results in the corresponding  $\text{NaHCO}_3$  concentrations from peak C % and N % in *N. salina* and *P. tricornutum*,  $7.49 \pm 0.04$  and  $12.95 \pm 0.62$  (Figure 4).

In the lipid formation phase the highest C % achieved: *N. salina*  $75.35 \pm 5.11$  and *P. tricornutum*  $112.48 \pm 0.45$  both in  $2.0 \text{ g L}^{-1}$   $\text{NaHCO}_3$  supplement. In the lipid phase the highest N % was in  $0.5 \text{ g L}^{-1}$   $\text{NaHCO}_3$  for both species. Although the highest C: N ratio in the LP resulted in the for *N. salina*,  $215.0 \text{ g L}^{-1}$   $\text{NaHCO}_3$ .  $09 \pm 0.32$ , while for *P. tricornutum* in  $2.0 \text{ g L}^{-1}$   $\text{NaHCO}_3$  at  $21.48 \pm 0.22$  (Figure 4).

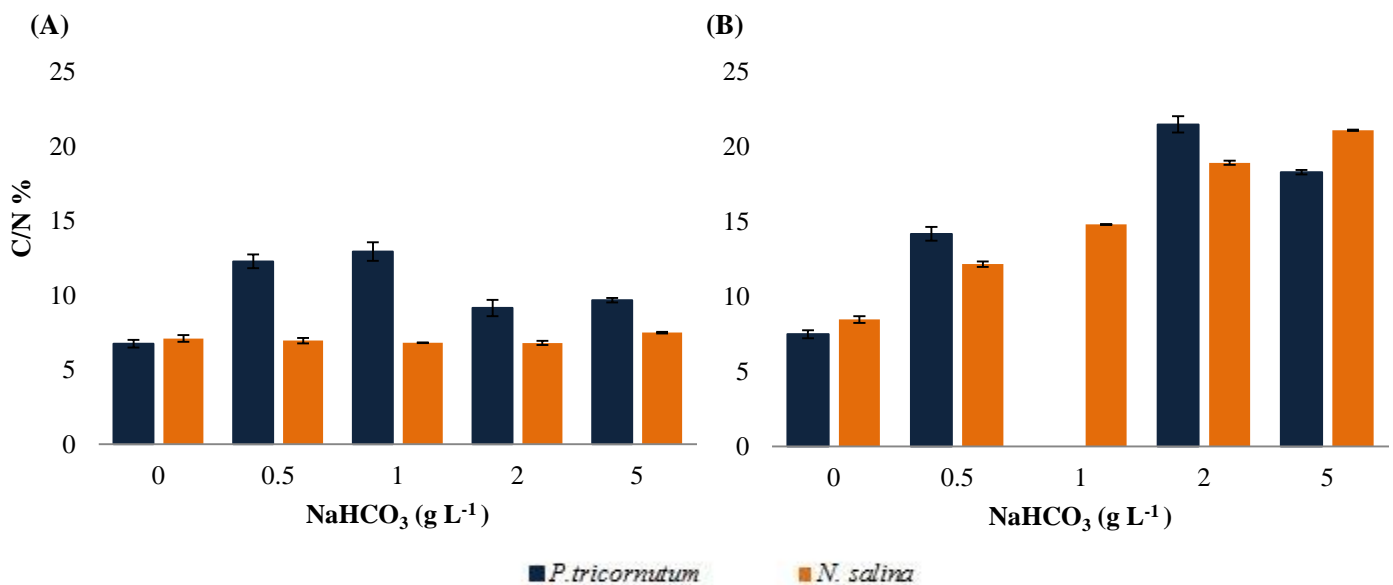


Figure 4: Carbon/Nitrogen (C:N) ratio during growth and lipid formation. (A) Growth phase C:N (B) Lipid phase C:N. Errors bars represent standard deviation (n=3). If the error bars are not visible, they are smaller than the symbol.

Table 2: Changes in Carbon (C %), Nitrogen (N %), and C: N ratio of *N. salina* and *P. tricornutum* from growth to lipid formation media. Errors bars represent standard deviation (n=3).

Species	Treatment									
	0 g L <sup>-1</sup> NaHCO <sub>3</sub>		0.5 g L <sup>-1</sup> NaHCO <sub>3</sub>		1 g L <sup>-1</sup> NaHCO <sub>3</sub>		2 g L <sup>-1</sup> NaHCO <sub>3</sub>		5 g L <sup>-1</sup> NaHCO <sub>3</sub>	
	GP	LP	GP	LP	GP	LP	GP	LP	GP	LP
<b>C %</b>										
<i>N. salina</i>	17.32 ± 0.53	33.12 ± 3.15	36.19 ± 1.76	68.80 ± 2.39	42.15 ± 2.19	65.03 ± 4.49	42.19 ± 2.77	75.35 ± 5.11	53.40 ± 3.32	75.16 ± 4.80
<i>P. tricornutum</i>	26.89 ± 2.58	36.80 ± 1.04	74.50 ± 2.87	86.89 ± 5.15	83.40 ± 3.00	—	56.27 ± 4.68	112.48 ± 0.45	51.54 ± 0.81	88.04 ± 8.21
<b>N %</b>										
<i>N. salina</i>	2.84 ± 0.16	4.56 ± 0.29	6.07 ± 0.14	6.61 ± 0.37	7.22 ± 0.40	5.13 ± 0.36	7.24 ± 0.62	4.66 ± 0.43	8.31 ± 0.49	4.16 ± 0.29
<i>P. tricornutum</i>	4.64 ± 0.39	5.74 ± 0.16	7.08 ± 0.42	7.15 ± 0.41	7.52 ± 0.11	—	7.17 ± 0.18	6.11 ± 0.07	6.22 ± 0.18	5.62 ± 0.60
<b>C:N</b>										
<i>N. salina</i>	7.10 ± 0.22	8.46 ± 0.26	6.96 ± 0.19	12.15 ± 0.25	6.81 ± 0.03	14.80 ± 0.50	6.80 ± 0.13	18.91 ± 0.61	7.49 ± 0.04	21.09 ± 0.32
<i>P. tricornutum</i>	6.75 ± 0.26	7.48 ± 0.16	12.28 ± 0.47	14.19 ± 0.20	12.95 ± 0.62	—	9.15 ± 0.54	21.48 ± 0.22	9.67 ± 0.15	18.29 ± 0.29

## Epifluorescence Microscope

Increased concentrations of NaHCO<sub>3</sub> indicate higher number of cells within culture when stained by Nile red for both *P. tricornutum* and *N. salina*. In *N. salina*, the concentration of NaHCO<sub>3</sub> displays a greater difference in cellular lipid storage from 0.0 g L<sup>-1</sup> to 5.0 g L<sup>-1</sup> NaHCO<sub>3</sub> (Figure 5A, 5B). In *P. tricornutum*, the cells demonstrated vibrant lipid content and highlighted the cellular lipid within the cell from 0.0 g L<sup>-1</sup> to 5.0 g L<sup>-1</sup> NaHCO<sub>3</sub> (Figure 6A, 6B).

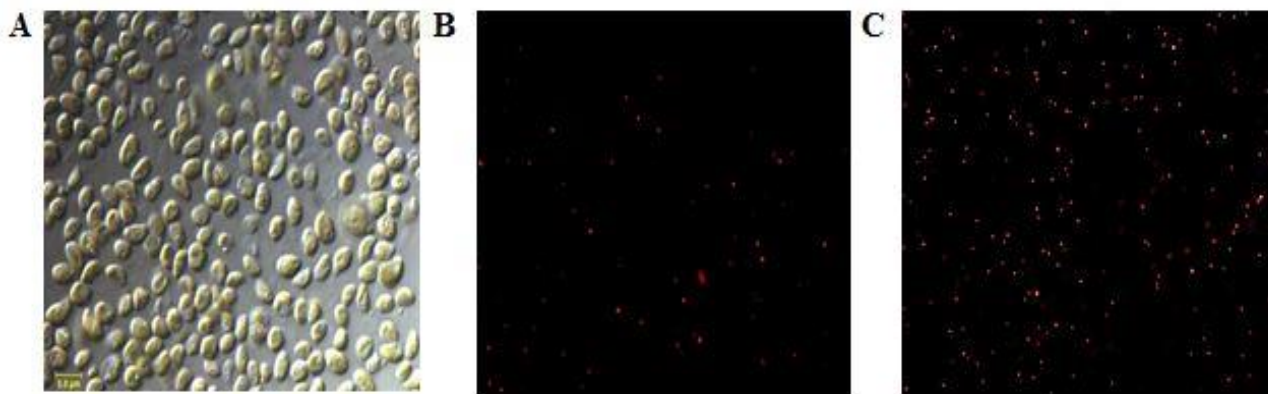


Figure 5: Photos of *N. salina* A) light microscope B)  $0.0 \text{ g L}^{-1} \text{ NaHCO}_3$  C)  $5.0 \text{ g L}^{-1} \text{ NaHCO}_3$

Figure 5A - Rossello, R. *Algae light up Industry*. 2010. Photograph. BIOPRO Baden-Württemberg  
 Figure 5B-C Nunez Marcella. Epifluorescence Microscope - *N. salina*. JPEG. Photograph.

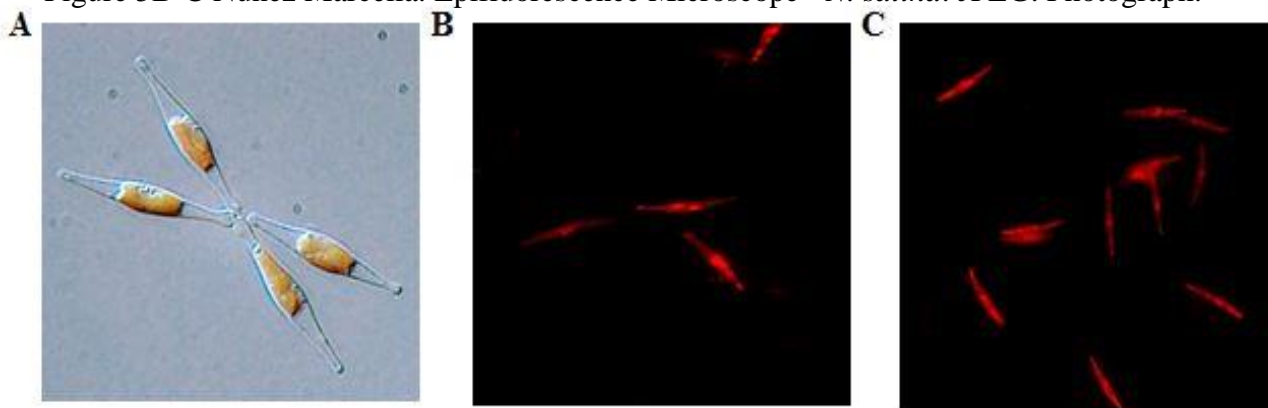


Figure 6: Photos of *P. tricornutum* A) light microscope B)  $0.0 \text{ g L}^{-1} \text{ NaHCO}_3$  C)  $5.0 \text{ g L}^{-1} \text{ NaHCO}_3$

Figure 6A - Bradbury, Jane. "Nature's nanotechnologists: unveiling the secrets of diatoms." *PLoS Biology* 2.10 (2004): e306. Photograph  
 Figure 6B-C Nunez Marcella. Epifluorescence Microscope- *P. tricornutum*. JPEG. Photograph.

### Lipid and Fatty Acid Composition

Of the fatty acids (FAMES) measured for *P. tricornutum*, palmitic acid (C16:0; saturated fatty acid, SFA) and palmitoleic acid (C16:1; monounsaturated fatty acid, MUFA) were estimated as the main components of total FAME (Table 3), whereas the myristic acid, linoleic acid, stearic acid, and oleic acid were presented as minor fatty acids only. The fatty acid profiles, as shown in

Table 3, indicated the presence of C14:0, C16:0, C16:1 cis, C18:0, C18:1, C18:2 trans, and C20:5. *N. salina* lipid profile included a more broader range of fatty acids (C:16 and C:18) compared to *P. tricornutum* (Table 3). The switch between growth and lipid phase for both species led to an increase in fatty acids. *N. salina* produced the highest oil index in higher concentrations of NaHCO<sub>3</sub>. The fatty acid components in *N. salina* were the highest in 2.0 g L<sup>-1</sup> and 5.0 g L<sup>-1</sup> NaHCO<sub>3</sub> treatments during the LP. As compared to *P. tricornutum* indicated an increase in lipids during the LP but not as significant as *N. salina* (Table 3).

Table 3: Fatty acid composition in % FAME of *N. salina* and *P. tricornutum* grown in media with different NaHCO<sub>3</sub> concentrations.

		<i>P. tricornutum</i>									
		0 g L <sup>-1</sup> NaHCO <sub>3</sub>		0.5 g L <sup>-1</sup> NaHCO <sub>3</sub>		1 g L <sup>-1</sup> NaHCO <sub>3</sub>		2 g L <sup>-1</sup> NaHCO <sub>3</sub>		5 g L <sup>-1</sup> NaHCO <sub>3</sub>	
Fatty Acid	Common Name	GP	LP	GP	LP	GP	LP	GP	LP	GP	LP
C14	Myristic acid	1.10 ± 0.82	8.01 ± 0.42	2.94 ± 0.93	5.52 ± 0.18	3.11 ± 0.35		3.60 ± 1.0	16.33 ± 1.24	4.86 ± 0.47	5.97 ± 0.40
C16	Palmitic acid	2.05 ± 1.54	9.93 ± 0.32	4.08 ± 1.32	7.37 ± 0.22	3.67 ± 0.09		4.17 ± 1.19	32.83 ± 2.62	6.99 ± 0.81	13.64 ± 1.03
C16:1 cis	Palmitoleic acid	4.63 ± 1.33	24.32 ±	10.75 ± 3.47	18.15 ± 0.42	11.91 ± 1.10		12.21 ± 3.3	70.10 ± 5.35	14.71 ± 1.37	29.76 ± 2.24
C18	Stearic acid							0.33 ± 0.001	0.74 ± 0.04		
C18:1	Oleic acid	0.90 ± 0.65	1.42 ± 0.11	3.24 ± 0.08	1.54 ± 0.06	3.15 ± 0.23		3.78 ± 1.05	7.70 ± 0.62	1.99 ± 0.45	2.78 ± 0.21
C18:2 trans	Linoleic acid		1.75 ± 0.001		1.01 ± 0.07			0.56 ± 0.26	2.77 ± 0.17	1.42 ± 0.20	1.30 ± 0.13
C20:5	EPA	3.96 ± 1.52	20.64 ± 0.22	5.06 ± 3.66	13.92 ± 0.38	7.48 ± 0.73		6.78 ± 2.23	25.11 ± 3.29	10.21 ± 1.56	11.34 ± 0.42

		<i>N. Salina</i>									
		0 g L <sup>-1</sup> NaHCO <sub>3</sub>		0.5 g L <sup>-1</sup> NaHCO <sub>3</sub>		1 g L <sup>-1</sup> NaHCO <sub>3</sub>		2 g L <sup>-1</sup> NaHCO <sub>3</sub>		5 g L <sup>-1</sup> NaHCO <sub>3</sub>	
Fatty Acid	Common Name	GP	LP	GP	LP	GP	LP	GP	LP	GP	LP
C14	Myristic acid						0.39 ± 0.10		0.81 ± 0.06		0.78 ± 0.04
C16	Palmitic acid	2.55 ± 0.04	4.84 ± 0.26	4.11 ± 0.16	13.20 ± 0.56	5.45 ± 0.95	24.83 ± 6.30	4.18 ± 1.15	55.34 ± 13.66	6.30 ± 0.22	61.26 ± 3.57
C16:1 cis	Palmitoleic acid				0.60 ± 0.01		1.08 ± 0.01		1.99 ± 0.25		1.62 ± 0.03
C16:1 trans	Palmitoleic acid								1.99 ± 0.25		1.62 ± 0.03
C16:3	Hexadecadienoic acid								18.02 ± 2.63		17.42 ± 0.92
C18	Stearic acid	0.27 ± 0.0	0.52 ± 0.08		1.58 ± 0.09	0.42 ± 0.06	3.70 ± 1.42	5.42 ± 0.0	16.35 ± 4.96	0.87 ± 0.08	18.13 ± 1.91
C18:1	Oleic acid		1.42 ± 0.14		8.12 ± 0.57		20.0 ± 6.69		62.36 ± 10.16	1.98 ± 0.08	79.34 ± 4.45
C18:3 trans	alpha-Linolenic acid	2.36 ± 0.09	4.99 ± 0.27	3.47 ± 0.15	8.40 ± 0.47	4.12 ± 1.55	15.30 ± 3.01	3.21 ± 1.37	29.97 ± 6.41	7.64 ± 0.22	35.58 ± 1.57
C18:3 cis	gamma-Linolenic acid	5.05 ± 0.3	9.67 ± 0.27	10.35 ± 0.93	13.82 ± 0.58	14.93 ± 1.85	18.47 ± 3.20	13.49 ± 4.97	30.40 ± 4.86	13.03 ± 0.39	28.56 ± 1.17
C20	Arachidic acid		1.27 ± 0.0	1.12 ± 0.13	1.43 ± 0.09	1.46 ± 0.27	2.03 ± 0.50	1.07 ± 0.32	3.50 ± 0.89	1.55 ± 0.06	3.35 ± 0.05

## CHAPTER IV

### DISCUSSION

An alternative source of inorganic carbon is important for regular photosynthesis and growth in microalgae in a biofuels setting where ambient CO<sub>2</sub> levels will not be sufficient because of the high mass/cell density of cultures. One way to provide carbon is the use of solid or dissolved sodium bicarbonate (NaHCO<sub>3</sub>) as a supplement in culture media. Interspecies differences in utilization of bicarbonate as a carbon source may result in differences in metabolic efficiency and biochemical composition (White *et al.*, 2012). This study examines the role of NaHCO<sub>3</sub> at various concentrations and the influence on growth and biochemical composition of two marine microalgae in both the growth and lipid phase of cultivation. The choice of microalgae for biofuels production requires a balance or tradeoffs between species which grow quickly against those which produce oil in large quantities. Further, given that most oil is produced during a “starvation” or “stress” phase, successful biofuels operations will require species which can be reliably manipulated, are tolerant of a range of environmental perturbations, natural and operator induced, and are able to “recover” from these alterations and continue growing (Jiang *et al.*, 2012). Stressful environmental conditions change the use of carbon uptake for proliferation to energy storage in the form of oil (Jiang *et al.*, 2012).

The investigation into growth phase responses showed varied behavior in *P. tricornutum* and *N. salina* cultures due to the utilization of NaHCO<sub>3</sub>. *P. tricornutum* cultures, specifically those grown with 0.5, 1.0 and 2.0 g L<sup>-1</sup> NaHCO<sub>3</sub> increased in biomass during the exponential phase of GP at similar rates and produced similar amounts of oil (intracellular neutral lipid bodies measured

with Nile red) than the control (Figure 3). Although after ~8 days, 5.0 g L<sup>-1</sup> NaHCO<sub>3</sub> increased over other treatments until the end of the GP exponential phase. According to a recent study, microalgal species have an optimum and threshold tolerance to NaHCO<sub>3</sub> addition, above which reduced cell densities/biomass are recorded (White *et al.*, 2012). This explanation of threshold tolerances may have been demonstrated in *P. tricornutum* highest NaHCO<sub>3</sub> concentration. .

Though the F<sub>v</sub>/F<sub>m</sub> (photosynthetic efficiency) decrease during the GP, it was not significant enough to indicate the phytoplankton were unhealthy. A good explanation in the decreased F<sub>v</sub>/F<sub>m</sub> values is self-shading within cell layers or too high of cell density in cultures (Figure 2A). As for *N. salina* growth rates during GP, there was an increased biomass concentrations from in order from 0.0 to 5.0 g L<sup>-1</sup> NaHCO<sub>3</sub> concentrations. The overall oil indices remained low and constant through the exponential phase showing no signs of stress, which can also be seen in the photosynthetic efficiency of *N. salina* (Figure 2C). In Table 1, it showed that *N. salina* and *P. tricornutum* have different responses to concentrations of NaHCO<sub>3</sub>. In comparing the marine species within each NaHCO<sub>3</sub> treatment, *P. tricornutum* produced the most protein including both crude protein and soluble protein (Table 1). It demonstrated that the protein production is strain specific and NaHCO<sub>3</sub> concentration dependent. In addition to the study the effect of NaHCO<sub>3</sub> concentrations on biomass production, cellular carbon and nitrogen were measured and C: N ratios. In the exponential phase of the GP, *N. salina* showed no variation within treatments, although *P. tricornutum* showed higher C: N ratio at lower NaHCO<sub>3</sub> concentrations (Figure 4A). However, when phytoplankton have a high growth rate, the C: N ratio decreases because the proportion of proteins increases (Rios *et al.*, 1998). In contrast, the proportion of storage compounds (carbohydrates and lipids) decreases. Conversely, the protein proportion decreases when the phytoplankton population is in stationary phase or cells become degraded (Rios *et al.*, 1998). In

relation to the oil indices, the fatty acid composition data during the growth phase showed no signs stress or strong indication of increased lipid formation for both marine species.

Under stressful environments microalgae slow down their cell division and remobilize carbon to producing energy storage products, e.g. lipids and/or starch in order to acclimate to the changed nutrient availability (Jiang *et al.*, 2012). Nitrogen limitation also reduces the ability of microalgae to use photosynthetically fixed carbon for protein synthesis (Berges *et al.*, 1996, Quigg *et al.*, 2012) without preventing the formation of photosynthetic storage products, which may result in the accumulation of lipids and/or carbohydrates depending on the species (Quigg *et al.*, 2012).

In the lipid phase of the research, there was a clear distinction on the effects of  $\text{NaHCO}_3$  concentrations amongst *N. salina* and *P. tricornutum*. In general, after transfer into N-free medium, cells continued to grow at a constant growth rates ( $\text{OD}_{750}$ ). Growth of *P. tricornutum* was not significantly different within the concentrations of  $\text{NaHCO}_3$ . It showed a similar trend in growth when compared to the growth phase with the  $0.5 \text{ g L}^{-1} \text{ NaHCO}_3$  maintaining the highest growth in the culture, followed by the  $2.0 \text{ g L}^{-1} \text{ NaHCO}_3$  (Figure1A). While *N. salina* overall growth rate surpass that of *P. tricornutum*, the trend changed slightly in the LP, maintaining the highest  $\text{OD}_{750}$  at  $5.0 \text{ g L}^{-1} \text{ NaHCO}_3$ , but  $0.5 \text{ g L}^{-1}$  it started to show an increase in later part of the exponential phase (~8 day) (Figure1D). These results on growth indicate a species-specific response to different concentrations of  $\text{NaHCO}_3$ . The  $F_v/F_m$  (photosynthetic efficiency) for both species maintained a ratio of  $0.50\text{-}0.530 \pm 0.032$ . Interestingly, the  $F_v/F_m$  of *P. tricornutum* significantly improved compare to the growth phase, possibly due to the lack of cellular self-

shading. The increase in  $F_v/F_m$  ratios may indicate an increased level of photosynthetic carbon fixation and increased metabolic activity demand. The stable  $F_v/F_m$  in both species under various  $\text{NaHCO}_3$  concentrations may indicate a high threshold tolerance level of  $\text{HCO}_3^-$  supplement. Increase in photosynthetic efficiency may suggest increased carbon fixation within the cultures.

In examining the oil indices from the LP, *N. salina* produced greater cellular lipids than the *P. tricornutum* while showing no signs of unstressed growth through the maximum quantum yield ( $F_v/F_m$ ). *N. salina* had highest Nile Red (NR) indices when grown at the highest  $\text{NaHCO}_3$  concentration ( $5.0 \text{ g L}^{-1}$ ; Figure 3D) that indicated an increase amount of cellular lipids. The research demonstrated that NR indices increased at maximum levels of  $\text{NaHCO}_3$  ( $0.5 \text{ g L}^{-1}$ ) but varies in lower concentrations, indicating a species-specific response to supplementation. In comparing both species in crude and soluble protein, *P. tricornutum* produced the highest concentrations but both species show a trend with increasing  $\text{NaHCO}_3$  supplementation gave higher concentrations in crude protein and decreased in values in soluble protein (Table 1). This may be due to the fact that both species were getting closer to the stationary phase and cells become degraded causing the protein proportion decrease. Furthermore, cellular carbon and nitrogen ratios (C:N) showed an increasing concentration trend along with the increasing  $\text{NaHCO}_3$  concentrations (Table 2) in both species. *P. tricornutum* demonstrated the higher values in C:N ratio compared to *N. salina*. The higher values of C: N ratios may be caused from the decrease of intracellular N content and the increase of intracellular carbon storage.

A large variation in fatty acid methyl esters (FAMES) was observed between both phases and treatments of  $\text{NaHCO}_3$  (Table 4). In general, highest overall lipid content was measured in *N.*



*salina* and *P. tricornutum* at  $5.0 \text{ g L}^{-1}$   $\text{NaHCO}_3$  during the lipid formation phase. The extent of lipid formation for *N. salina* significantly exceeded *P. tricornutum* and showed large difference between N-replete (GP) and N-free (LP) media (Table 3), which far exceeded expectations. The study found that increased lipid accumulation can be associated at higher levels of  $\text{NaHCO}_3$  but is species dependent according to FAMES concentrations (Table 3). The fatty acid profiles, as shown in Table 3, indicated a varied the presence of C14:0, C16:0, C16:1 cis, C18:0, C18:1, C18:2 trans, and C20:5 between *P. tricornutum* and *N. salina* in growth and lipid phase. The two most important properties of fatty acids that affect the fuel properties are the length of the carbon chain and the number of double bonds. Oils that could potentially be used to produce biodiesel vary greatly in these properties (Stansell *et al*, 2011). The ideal biodiesel feedstock would be composed entirely of C16:1 and C18:1 MUFAs (Knothe 2008), so in practice a biodiesel feedstock should have concentrations of C16:1 and C18:1 that are as high as possible and therefore keep the concentrations of all other fatty acids as low as possible (Stansell *et al*, 2011). The reasons of lipid accumulation in response to  $\text{NaHCO}_3$  and N-limitation stress have not been demonstrated long in experimental research. There has been no general agreement on the mechanisms by which  $\text{NaHCO}_3$  contributes to overall cultivation of microalgae and how it might affect the key parameters, such as algal growth, biomass productivity and lipid production.

The present findings in this research are unique, as the focus on the additional supplement of  $\text{NaHCO}_3$  as alternative source for carbon and how it affects the factors on growth and lipid composition. These findings reinforce the idea of species-specific responses and agree with other studies (White *et al*, 2012).

Another unique aspect of algae is the potential of various species that can be used to optimize the production of different biofuels or bioproducts. In this research, *N. salina* demonstrated to be a good candidate in lipid formation for use in biofuel production. On the other hand algae offers a diverse spectrum of valuable products, such as food, nutritional compounds, omega-3 fatty acids, animal feed, and recombinant proteins (Pienkos *et al.*, 2009). Although, *P. tricornutum* in past studies has shown to be a good oil producer, in this study the marine species demonstrated a greater increase in protein production than lipids with increasing concentrations of  $\text{NaHCO}_3$ . In this situation, *P. tricornutum* proves to be a more beneficial choice for algal bioproducts. Furthermore, rapid growth and high oil content can be promoted through  $\text{NaHCO}_3$  addition at certain concentrations in microalgal species as an alternative to the addition of gaseous  $\text{CO}_2$  used in the biofuel industry.

## REFERENCES

- Achara, N. Biofuel from algae. *The Journal of American Science* 8.1 (2012): 240-244.
- Berges J.A., Falkowski P.G., Physiological stress and cell death in marine phytoplankton: induction of proteases in response to nitrogen or light limitation, *Limnol. Oceanogr.* 43 (1998) 129-135.
- Berges J.A., Charlebois D.O., Mauzerall D.C., Falkowski P.G., Differential effects of nitrogen limitation on photosynthetic efficiency of photosystems I and II in microalgae, *Plant Physiol.* 110 (1996) 689-696.
- Britton LJ, Greeson PE, editors. *Methods for collection and analysis of aquatic biological and microbiological samples: U.S. Geological Survey Techniques of Water-Resource Investigations.* Washington, DC; 1987.
- Chisti, Y. Biodiesel from microalgae beats bioethanol. *Trends in biotechnology* 26.3 (2008): 126-131.
- Chisti Y. Biodiesel from microalgae. *Biotechnol Adv* (2007);25:294.
- Christie WW. *Lipid Analysis: Isolation, Separation, Identification, and Structural Analysis of Lipids.* 3rd ed. Bridgwater, England: The Oily Press; (2003).
- Cooksey KE, Guckert JB, Williams SA, Callis PR. Fluorometric determination of the neutral lipid content of microalgal cells using Nile Red. *J Microbiol Meth* (1987);6:333.
- Dahmer M, Fleming P, Collins G, Hildebrand D. A rapid screening technique for determining the lipid composition of soybean seeds. *J Am Oil Chem Soc* (1989);66:543.
- Dean A.P., Sigeo D.C., Estrada B., Pittman J.K., Using FTIR spectroscopy for rapid determination of lipid accumulation in response to nitrogen limitation in freshwater microalgae, *Bioresour. Technol.* 101 (2010) 4499-4507.
- Demirbas, Ayhan, and M. Fatih Demirbas. Importance of algae oil as a source of biodiesel. *Energy Conversion and Management* 52.1 (2011): 163-170.

- Elsley D, Jameson D, Raleigh B, Cooney MJ. Fluorescent measurement of microalgal neutral lipids. *J Microbiol Meth* (2007): 68:639.
- Geider R.J., La Roche J., Greene R.M., Olaizola M., Response of the photosynthetic apparatus of *Phaeodactylum tricornutum* (Bacillariophyceae) to nitrate, phosphate, or iron starvation, *J. Phycol.* 29 (1993) 755-766.
- Glaser C, Demmelmair H, Koletzko B. High-Throughput Analysis of Total Plasma Fatty Acid Composition with Direct *In Situ* Transesterification. *Plos One* 2010;5:12045.
- Giordano M.,Kansiz M., Heraud P., Beardall J., Wood B., McNaughton D., Fourier transform infrared spectroscopy as a novel tool to investigate changes in intracellular macromolecular pools in the marine microalga *Chaetoceros muellerii* (Bacillariophyceae), *J. Phycol.* 37 (2001): 271-279.
- Guillard RRL, Ryther JH. Studies of marine planktonic diatoms. I. *Cyclotella nana* Hustedt and *Detonula confervacea* (Cleve) Gran. *Can J Microbiol* (1962): 8:229.
- Guillard RLL. Division rates. In: Stein JR (ed) *Handbook of Phycological Methods: Culture Methods and Growth Measurements*. Cambridge University Press, Cambridge, (1973) 289-311
- Gunawan S, Maulana S, Anwar K, Widjaja T. Rice bran, a potential source of biodiesel production in Indonesia. *Ind Crop Prod* (2011): 33:624.
- Hannon, M., Gimpel, J., Tran, M., Rasala, B., Mayfield, S. Biofuels from algae: challenges and potential. *Biofuels* 1.5 (2010): 763-784.
- Heydeman MT. Aspects of protein production by unicellular organisms. In: Jones JGW, editor. *The Biological Efficiency of Protein Production*: Cambridge University Press; ( 1973), p. 303.

- Jiang Y, Yoshida T, Quigg A. Photosynthetic performance, lipid production and biomass composition in response to nitrogen limitation in marine microalgae *Plant Physiol Biochem* (2012);54:8.
- Knothe G., “Designer” biodiesel: optimizing fatty ester composition to improve fuel properties. *Energy Fuels* (2008): 22:1358–1364
- Lepage G, Roy CC. Specific methylation of plasma nonesterified fatty acids in a one-step reaction. *J Lipid Res* 1988;29:227.
- O’Fallon JV, Busboom JR, Nelson ML, Gaskins CT. A direct method for fatty acid methyl ester synthesis: Application to wet meat tissues, oils, and feedstuffs. *J Anim Sci* (2007): 85:1511.
- Parkhill J.P., Maillet G., Cullen J.J., Fluorescence-based maximal quantum yield for PSII as a diagnostic of nutrient stress, *J. Phycol.* 37 (2001): 517-529.
- Peydecastaing J, Vaca-Garcia C, Borredon E. Accurate determination of the degree of substitution of long chain cellulose esters. *Cellulose* 2009;16:289.
- Pienkos PT, Darzins A. The promise and challenges of micro-algal derived biofuels. *Biofuel Bioproducts Biorefin* 3 (2009): 431–440
- Revellame E, Hernandez R, French W, Holmes W, Alley E. Biodiesel from activated sludge through in situ transesterification. *J Chem Tech Biotechnol* (2010): 85:614.
- Ríos, A. F., Fraga, F., Pérez, F. F., Figueiras, F. G. Chemical composition of phytoplankton and Particulate Organic Matter in the Ría de Vigo (NW Spain). (1998).
- Singh J., Gu S. Commercialization potential of microalgae for biofuels production. *Renewable and Sustainable Energy Reviews* 14.9 (2010): 2596-2610.
- Stansell, R.G, Gray M.G., Stuart D.S. Microalgal fatty acid composition: implications for biodiesel quality. *Journal of Applied Phycology* 24.4 (2012): 791-801.

Zhu C, Lee Y. Determination of biomass dry weight of marine microalgae. *J Appl Phycol* 1997;9:189